Macromolecules

Article

Synthesis and Electrochemical Properties of Novel Aromatic Poly(amine#amide)s with Anodically Highly Stable Yellow and Blue Electrochromic Behaviors

Guey-Sheng Liou, and Hung-Yi Lin

Macromolecules, **2009**, 42 (1), 125-134 • DOI: 10.1021/ma8021019 • Publication Date (Web): 08 December 2008

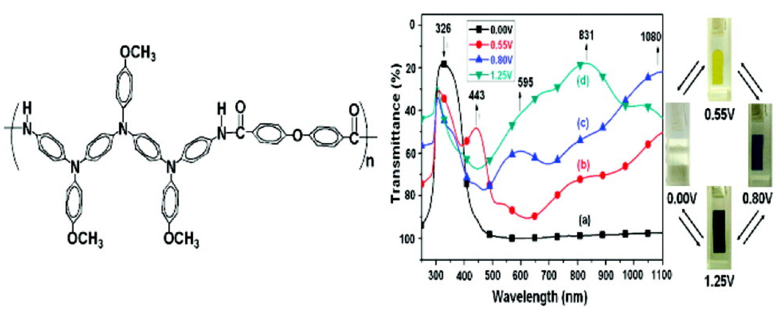

Macromolecules is published by the American Chemical Society. 1155 Sixteenth Street N.W., Washington, DC 20036

Synthesis and Electrochemical Properties of Novel Aromatic Poly(amine−amide)s with Anodically Highly Stable Yellow and Blue Electrochromic Behaviors

Guey-Sheng Liou*,† and Hung-Yi Lin‡

Institute of Polymer Science and Engineering, National Taiwan University, No. 1, Sec. 4, Roosevelt Rd. Taipei, 10617, Taiwan, and Department of Applied Chemistry, National Chi Nan University, 1 University Rd. Puli, Nantou Hsien, 54561, Taiwan

Received September 16, 2008; Revised Manuscript Received November 8, 2008

ABSTRACT: A new triphenylamine-containing aromatic diamine, 4,4′-bis[4-aminophenyl(4-methoxyphenyl)amino)]-4″-methoxytriphenylamine (**5**), was successfully synthesized by the Ullmann reaction of 4,4′-dibromo-4″-methoxytriphenylamine (**2**) with 4-methoxy-4′-nitrodiphenylamine (**3**), followed by palladium-catalyzed hydrazine reduction of the dinitro (**4**) intermediate. A series of novel polyamides having inherent viscosities of 0.22−0.64 dL/g were prepared via the direct phosphorylation polycondensation from the diamine and various dicarboxylic acids. All the polymers were amorphous with good solubility in many organic solvents, such as *N*-methyl-2-pyrrolidinone (NMP) and *N*,*N*-dimethylacetamide (DMAc), and could be solution-cast into polymer films. These aromatic polyamides had useful levels of thermal stability associated with their relatively high softening temperature (200−244 °C), 10% weight-loss temperatures in excess of 460 °C, and char yields at 800 °C in nitrogen higher than 55%. The hole-transporting and electrochromic properties are examined by electrochemical and spectroelectrochemical methods. Oxidation of compound **4** was proved by using an optically transparent thin-layer electrode (OTTLE) cell coupled with UV−vis/NIR spectroscopy. Reversibility of the first oxidation was up to 99%, second oxidation was 94%, and third oxidation was 80%. Polyamide **Ic** shows the reversibility of the first oxidation was up to 100%, second oxidation was 99%, and third oxidation was 75%. Cyclic voltammograms of the polyamide films cast onto an indium−tin oxide (ITO)-coated glass substrate exhibited three reversible oxidation redox couples ($E_{1/2}$) at 0.39−0.47, 0.64−0.72, and 1.02−1.13 V vs Ag/AgCl in acetonitrile solution, and polyamide **Ie** showed additional fourth reversible oxidation redox couples at 1.07 V. The polyamide films revealed excellent reversible stability of anodic electrochromic characteristics with a color change from the colorless or pale yellowish neutral form to yellow and blue oxidized form at applied potentials ranging from 0.00 to 0.80 V. These electrochromic materials not only showed good coloration efficiency of yellow (CE = 203 cm^2/C) and blue (CE = 194 cm^2/C) but also exhibited high contrast of optical transmittance change (ΔT %) up to 59% at 443 nm for yellow and 79% at 1080 nm for blue. After over 500 cyclic switches, the polymer films still exhibited excellent stability of electrochromic characteristics.

Introduction

Electrochromism is defined as a reversible and visible change in the transmittance of a material as the result of an electrochemical oxidation or reduction.[1] These electroactive species change their optical absorption bands due to the gain or loss of an electron depending on their cathodic or anodic character. Color changes are commonly between a transparent state, where the chromophore only absorbs in the UV region, and a colored state or between two colored states in a given electrolyte solution. The electrochromic material may exhibit several colors in different oxidation or reduction state. This property was so interesting and has been largely studied for different technological applications, such as construction of mirrors,[2] electrochromic displays,[3] smart windows,[4] and earth-tone chameleon materials.[5] The first study and commercial interests in electrochromic materials started with inorganic compounds such as tungsten trioxide (WO_3) and iridium dioxide (IrO_2).[6] Then, the organic materials such as viologens, metallophthalocyanines, and conducting polymers have recently received much attention for cathodic electrochromic applications[7] because of the different colors observed while switching among their different redox states.[8] Conducting polymers (CPs) have several advantages over inorganic compounds; these show outstanding coloration efficiency, fast switching ability,[9] multiple colors with the same material,[10] and fine-tuning of the band gap (and the color) through chemical structure modification.[11] But they have some inherent drawbacks, such as lack of film uniformity over large surface, low material recovery and stability to environments, and irregular linkages within the polymer backbone.

The characteristic structure feature of triphenylamine (TPA) is the nitrogen center, the electroactive site of TPA, which is linked to three electron-rich phenyl groups in a propeller-like geometry. The anodic oxidation pathways of TPA were well studied.[12] In 1966, Adams and co-workers reported the electrogenerated cation radical of $TPA^{\bullet +}$ is not stable and could form tetraphenylbenzidine (TPB), which is more easily oxidized than the TPA molecule. However, when the phenyl groups were incorporated by electron-donating substituents at the *para* position of TPA, the coupling reactions were greatly prevented by affording stable cationic radicals.[13]

Wholly aromatic polyamides are characterized as highly thermally stable polymers with a favorable balance of physical and chemical properties. However, the rigidity of the backbone and strong hydrogen bonding result in high melting temperatures or glass-transition temperatures and limited solubility in most organic solvents.[14] The properties make them generally intractable or difficult to process, thus restricting their applications in some fields. To overcome these limitations, polymer-structure modification becomes necessary. One of the common approaches for increasing the solubility and processability of aromatic polymers without sacrificing high thermal stability is

* Corresponding author. E-mail: gsliou@ntu.edu.tw.
† National Taiwan University.
‡ National Chi Nan University.

10.1021/ma8021019 CCC: $40.75
Published on Web 12/08/2008

Scheme 1. Synthesis of Monomers

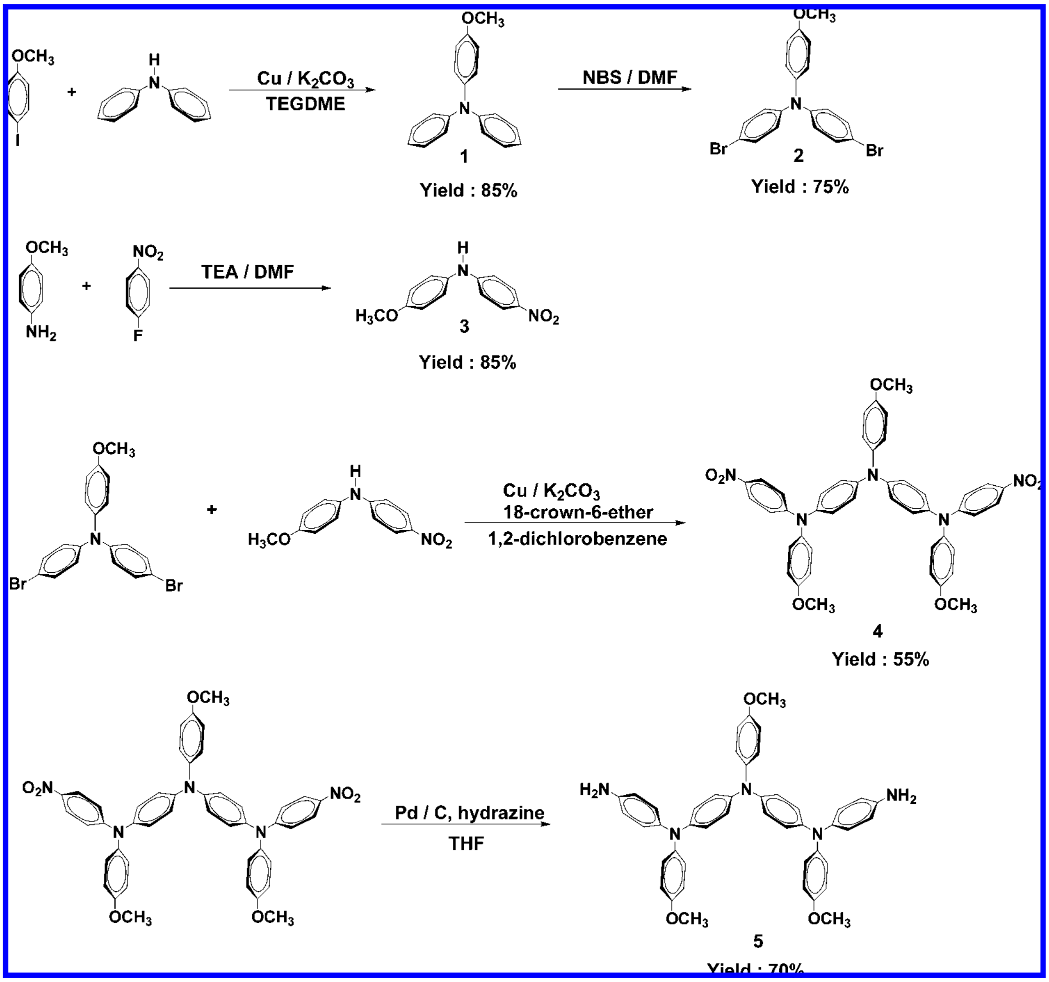

the introduction of bulky, packing-disruptive groups into the polymer backbone.[15] Recently, we have reported some TPA-containing polyamides and polyimides.[16] Because of the incorporation of bulky, three-dimensional TPA units along the polymer backbone, all the polymers were amorphous and exhibited good solubility in many aprotic solvents with excellent thin-film-forming capability. Triarylamine-based polymers are not only widely used as the hole-transport layer in electroluminescent devices but also show electrochromic behavior. Recently, we have initiated a study to obtain TPA-containing anodic electrochromic polymers which exhibited green and blue colors in the oxidized state and were transparent in the neutral state.[17] In order to be useful for applications, electrochromic materials must exhibit long-term stability, multiple colors with the same material, and large changes in transmittance (large ΔT %) between their bleached and colored states.[18] Our strategy is to synthesize the *N,N,N′,N′*-tetrasubstituted-1,4-phenylenediamines monomers such as diamine and dicarboxylic acids that phenyl groups were incorporated by electron-donating substituents at the *para* position of TPA; the coupling reactions were greatly prevented by affording stable cationic radicals and lowering the oxidation potentials. The corresponding polymers with high molecular weights and high thermal stability could be obtained through conventional direct polycondensation techniques. Because of the incorporation of packing-disruptive, propeller-shaped TPA units along the polymer backbone, most of these polymers exhibited good solubility in polar organic solvents, and uniform, transparent amorphous thin films could be obtained by solution-casting and spin-coating methods, which are advantageous for their ready fabrication of large-area, thin-film devices.

In this article, we therefore synthesized a new diamine, 4,4′-bis[4-aminophenyl(4-methoxyphenyl)amino]-4″-methoxytriphenylamine (**5**), and its derived polyamides containing TPA groups with an electron-rich pendent 4-methoxyphenyl ring which permits tuning the colors and redox potential of the polymers. The characterizations such as solubility, thermal, electrochemical, and optical properties were investigated.

Experimental Section

Materials. Diphenylamine (99%, ACROS), 4-fluoronitrobenzene (99%, ACROS), 4-iodoanisole (98%, ALFA AESAR), *N*-bromosuccinimide (99%, ACROS), 4-methoxyaniline (99%, ACROS), triethylamine (TEDIA), copper powder (99% ACROS), potassium carbonate (SCHARLAU), 18-crown-6 ether (TCI), triethylene glycol dimethyl ether (TEGDME) (99%, ALFA AESAR), 10% Pd/C, *o*-dichlorobenzene (TEDIA), toluene (TEDIA), *N,N*-dimethylacetamide (DMAc) (TEDIA), *N,N*-dimethylformamide (DMF) (ACROS), *N*-methyl-2-pyrrolidinone (NMP) (TEDIA), chloroform ($CHCl_3$) (TEDIA), and tetrahydrofuran (THF) (ECHO) were used without further purification. Tetrabutylammonium perchlorate (TBAP) was obtained from ACROS and recrystallized twice from ethyl acetate and then dried *in vacuo* prior to use. All other reagents were used as received from commercial sources.

Polymer Synthesis. The synthesis of polyamide **Ic** is used as an example to illustrate the general synthetic route. The typical procedure was as follows. A mixture of 0.35 g (0.5 mmol) of the diamine (**5**), 0.13 g (0.5 mmol) of 4,4′-dicarboxydiphenyl ether, 0.06 g of calcium chloride, 0.5 mL of TPP, 0.25 mL of pyridine,

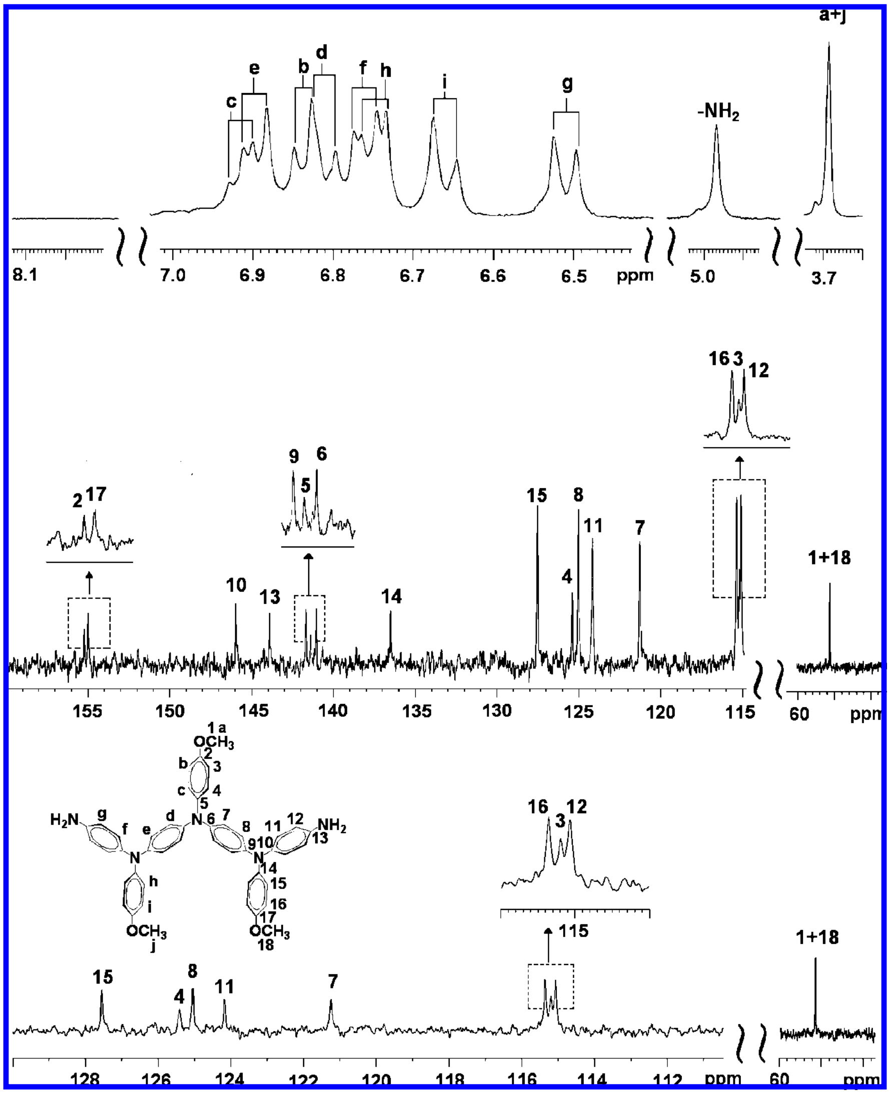

Figure 1. ^{1}H, ^{13}C, and DEPT135 NMR of compound **5** in DMSO-d_6.

Scheme 2. Synthesis of Polyamides by Direct Polycondesation Reaction

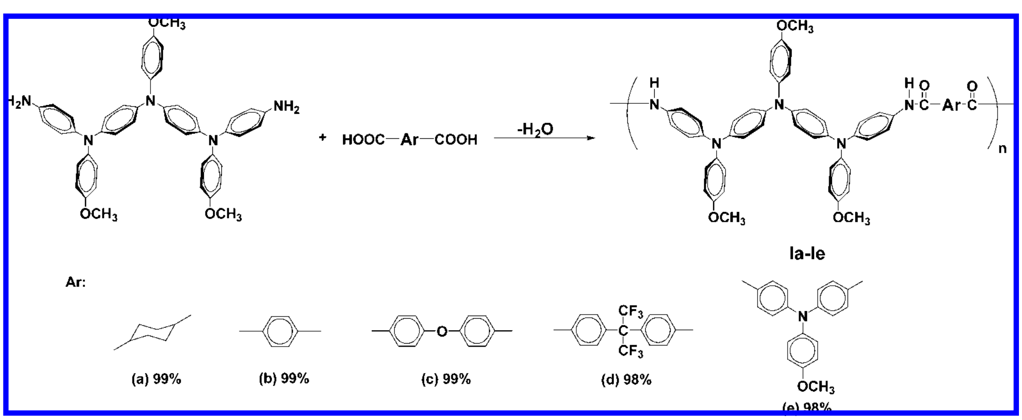

and 0.7 mL of NMP was heated with stirring at 105 °C for 3 h. The polymer solution was poured slowly into 300 mL of stirring methanol, giving rise to a stringy, fiberlike precipitate that was collected by filtration, washed thoroughly with hot water and methanol, and dried at 100 °C; yield: 0.46 g (99%). Reprecipitations from DMAc into methanol were carried out twice for further purification. The IR spectrum of **Ic** (film) exhibited characteristic amide absorption bands at 3306 cm^{-1} (N−H stretch) and 1656 cm^{-1} (amide carbonyl). Anal. Calcd for **Ic** $(C_{59}H_{47}N_5O_7)_n$ $(922.03)_n$: C, 76.86%; H, 5.14%; N, 7.60%. Found: C, 75.26%; H, 5.23%; N, 7.43%. **Id**: ^{1}H NMR (DMSO-d_6, δ, ppm): 3.70 (s, 9H, −OCH$_3$), 6.83−7.05 (m, 24H), 7.47 (d, 4H), 7.62 (d, 4H), 7.98 (d, 4H), 10.35 (s, 2H, NH−CO). The other polyamides were prepared by an analogous procedure.

Measurements. Infrared spectra were recorded on a Perkin-Elmer RXI FT-IR spectrometer. Elemental analyses were run in an Elementar VarioEL-III. ^{1}H NMR and ^{13}C NMR spectra were measured on a Bruker AV-300 FT-NMR system. A Finnigan LCQ

Table 1. Solubility and GPC Data of Polyamides

					solvent[d]					
code	η_{inh}[a]	M_w[b]	M_n[b]	PDI[c]	NMP	DMAc	DMSO	DMF	THF	$CHCl_3$
Ia	0.64	28 400	13 900	2.03	+	+	±	±	−	−
Ib	0.58	−	−	−	+	+	±	−	−	−
Ic	0.47	24 500	11 300	2.16	+	+	±	±	−	−
Id	0.42	21 600	13 400	1.61	++	+	±	±	−	
Ie	0.22	21 800	10 300	2.12	++	++	+	+	++	−

[a] Measured at a polymer concentration of 0.5 g/dL in NMP at 30 °C. [b] Average molecular weights relative to polystyrene standard in DMF by GPC. [c] PDI = M_w/M_n. [d] ++, soluble at room temperature; +, soluble on heating; ±, soluble on heating, but some precipitate produced after cooling; −, insoluble even on heating.

Advantage MAX LC/MS/MS ion trap mass spectrometer (ESI-MS; Thermo Finnigan, San Jose, CA) was used in the electrospray ionization (ESI) mode. The spray voltage was 2.4 kV with a current of about 20 mA. Samples were introduced to the source by direct insert probe. The inherent viscosities were determined at 0.5 g/dL concentration using a Tamson TV-2000 viscometer at 30 °C. Wide-angle X-ray diffraction (WAXD) measurements were performed at room temperature (ca. 25 °C) on a Shimadzu XRD-7000 X-ray diffractometer (40 kV, 20 mA), using graphite-monochromatized Cu Kα radiation. Ultraviolet−visible (UV−vis) spectra of the polymer films were recorded on a Varian Cary 50 Probe spectrometer. Gel permeation chromatography (GPC) was carried out on a Waters chromatography unit interfaced with a Waters 2410 refractive index detector. Two Waters 5 μm Styragel HR-2 and HR-4 columns (7.8 mm i.d. × 300 mm) connected in series were used with DMF as the eluent at a flow rate of 1 mL/min and were calibrated with narrow polystyrene standards. Thermogravimetric analysis (TGA) was conducted with a PerkinElmer Pyris 1 TGA. Experiments were carried out on approximately 6−8 mg film samples heated in flowing nitrogen or air (flow rate = 20 cm^3/min) at a heating rate of 20 °C/min. DSC analyses were performed on a PerkinElmer Pyris Diamond DSC at a scan rate of 20 °C/min in flowing nitrogen (20 cm^3/min). Thermomechanical analysis (TMA) was conducted with a PerkinElmer TMA 7 instrument. The TMA experiments were conducted from 50 to 300 °C at a scan rate of 10 °C/min with a penetration probe 1.0 mm in diameter under an applied constant load of 50 mN. Cyclic voltammetry was performed with a Bioanalytical System Model CV-27 potentiostat, and a BAS *X*−*Y* recorder with ITO (polymer films area about 0.7 cm × 0.5 cm) was used as a working electrode and a platinum wire as an auxiliary electrode at a scan rate of 50 mV/s against a Ag/AgCl reference electrode in solution of 0.1 M tetrabutylammonium perchlorate (TBAP)/acetonitrile (CH_3CN). Voltammograms are presented with the positive potential pointing to the left and with increasing anodic currents pointing downward. The spectroelectrochemical cell was composed of a 1 cm cuvette, ITO as a working electrode, a platinum wire as an auxiliary electrode, and an Ag/AgCl reference electrode. Absorption spectra in spectroelectochemical analysis were measured with a HP 8453 UV−vis and Jasco V-570 UV−vis/NIR spectrophotometer. Photoluminescence spectra were measured with a Jasco FP-6300 spectrofluorometer. Fluorescence quantum yields (Φ_F) of polyamides in NMP was measured by using quinine sulfate in 1 N H_2SO_4 as a reference standard (Φ_F = 0.546).[19] All corrected fluorescence excitation spectra were found to be equivalent to their respective absorption spectra.

Results and Discussion

Monomer Synthesis. Compound **5** was synthesized by the Ullmann reaction of 4,4′-dibromo-4″-methoxytriphenylamine (**2**) with 4-methoxy-4′-nitrodiphenylamine (**3**), followed by palladium-catalyzed hydrazine reduction of compound **4** and the synthetic route outlined in Scheme 1. Elemental analysis, IR, ^{1}H NMR, and ^{13}C NMR spectroscopic techniques were used to identify structures of the intermediate compounds **1**−**4** and the target diamine monomer **5**. Figure S1 shows the FTIR spectra of the compounds **4** and **5** and polyamide **Ic**. The nitro group of compound **4** gave two characteristic bands at around 1585 and 1322 cm^{-1} (−NO_2 asymmetric and symmetric stretching). After reduction, the characteristic absorptions of the nitro group disappeared, and the amino group showed the typical N−H stretching absorption of 3462 and 3347 cm^{-1}. Figure 1 illustrates the ^{1}H, ^{13}C, and DEPT135 NMR spectra of the diamine monomer **5**. Assignment of each proton is assisted by the two-dimensional NMR spectra shown in Figure S8. The spectra agree well with the proposed molecular structure of compound **5**. The ^{1}H NMR spectra confirm that the nitro groups have been completely transformed into amino groups by the high field shift of the aromatic protons and the resonance signals at around 4.97 ppm, corresponding to the amino protons. Figures S1−S7 illustrated the FTIR, ^{1}H NMR, and ^{13}C NMR spectra of intermediate products **1**−**4**.

Polymer Synthesis. According to the phosphorylation technique first described by Yamazaki and co-workers,[20] a series of novel polyamides **Ia**−**Ie** were synthesized from the diamine **5** and various dicarboxylic acids via solution polycondensation using triphenyl phosphite and pyridine as condensing agents, as shown in Scheme 2. All the polymerization proceeded homogeneously throughout the reaction and afforded clear and highly viscous polymer solutions, which precipitated in a tough, fiberlike form when the resulting polymer solutions were slowly poured into stirring methanol. As shown in Table 1, the obtained polyamides had inherent viscosities in the range of 0.22−0.64 dL/g. The molecular weights were measured by GPC using polystyrenes as standard and DMF as eluent. **Ia** and **Ic**−**Ie** had the weight-average molecular weight (M_w) of 21 800−28 400 and polydispersity index (M_w/M_n) of 1.61−2.16. These polymers could be solution-cast into films, indicating the formation of high molecular weight polymers.

The elemental analyses were in a good agreement with the proposed structures. The formation of polyamides was also confirmed by IR and NMR spectroscopy. Figure S1 shows a typical IR spectrum for polyamide **Ic**. The characteristic IR absorption bands of the amide group were around 3306 cm^{-1} (N−H stretching) and 1656 cm^{-1} (amide carbonyl). Figure 2 shows a typical set of ^{1}H NMR spectra of polyamide **Id** in DMSO-d_6. All the peaks could be readily assigned to the hydrogen and had the correct number of hydrogen atoms in the repeating unit. The resonance peak appearing at 10.35 ppm in the ^{1}H NMR spectrum also supports the formation of amide linkages.

Basic Characterization. The solubility behavior of polyamides **Ia**−**Ie** was tested qualitatively, and the results are summarized in Table 1. All the polyamides were highly soluble in polar solvents such as NMP, DMAc, and DMF, and the enhanced solubility could be attributed to the introduction of the bulky pendent methoxy-substituted TPA moiety into the repeat unit. Thus, the excellent solubility makes these polymers potential candidates for practical applications by spin- or dip-coating processes. The wide-angle X-ray diffraction (WAXD) patterns of the polyamides given in Figure S10 indicate that the polymers were essentially amorphous. The thermal properties of the polyamides were investigated by TGA, DSC, and TMA. The results are summarized in Table 2, and typical TGA and TMA curves of representative polyamide **Ic** are shown in Figure 3. All the aromatic polyamides exhibited good thermal stability, and their 10% weight-loss temperatures in nitrogen and air were recorded at 460−500 and 455−495 °C, respectively. The char yield of these aromatic polymers was more than 55% at 800 °C in a nitrogen atmosphere. The high char yields of these polymers could be ascribed to their high aromatic content. The softening temperature (T_s) values of the polymer films were determined from the onset temperature of the probe displacement

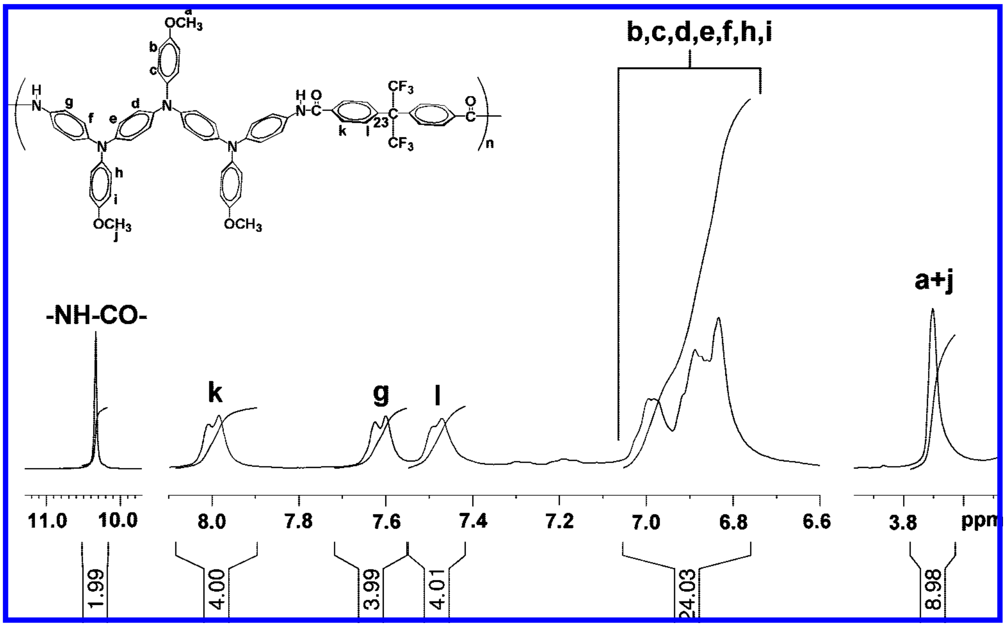

Figure 2. ^{1}H NMR of polyamide **Id** in DMSO-d_6.

Table 2. Thermal Properties of Polyamides

code	T_g (°C)[a]	T_s (°C)[b]	T_d at 5% weight loss[c]		T_d at 10% weight loss[c]		char yield weight (%)[d]
			N_2	air	N_2	air	
Ia	220	235	440	435	460	455	59
Ib	233	233	455	450	480	480	63
Ic	221	229	460	455	490	490	63
Id	244	244	465	455	500	495	63
Ie	200	198	460	455	480	475	55

[a] Midpoint temperature of baseline shift on the DSC heating trace (rate 20 °C/min). [b] Softening temperature measured by TMA with a constant applied load of 50 mN at a heating rate of 10 °C/min. [c] Decomposition temperature, recorded via TGA at a heating rate of 20 °C/min and a gas-flow rate of 20 cm^3/min. [d] Residual weight percentage at 800 °C in nitrogen.

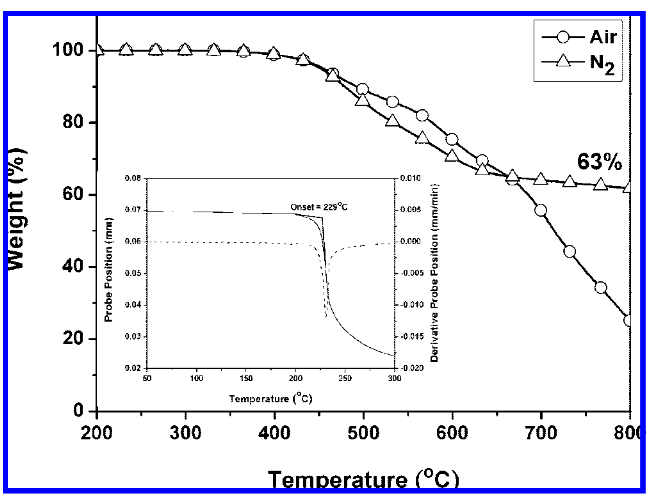

Figure 3. TGA and TMA curves of polyamide **Ic** (TGA: at a scan rate of 20 °C/min; TMA: heating rate of 10 °C/min).

on the TMA trace. The T_g observed in the range of 198−244 °C for these polymers could be easily measured by the DSC thermograms.

Optical and Electrochemical Properties. The optical and electrochemical properties of the monomers (compounds **4** and **5**) and polyamides **Ia**−**Ie** were investigated by UV−vis and photoluminescence spectroscopy as well as cyclic voltammetry. The results are summarized in Table 3 and Table S1. The UV−vis absorption of **Ia** and **Ic** (Figure 4) exhibited strong absorption at 315 and 333 nm in NMP solutions, which are assignable to a $\pi-\pi^*$ transition resulting from the conjugation between the aromatic rings and nitrogen atoms. The UV−vis absorption of polyamide films **Ia**−**Ie** also showed similar single absorption at 320−339 nm. Aromatic−aliphatic polyamide **Ia** in NMP exhibited fluorescence emission maxima at 431 nm with quantum yields 2.26%. The higher fluorescence quantum yield of aromatic−aliphatic polyamide **Ia** compared with aromatic polyamides **Ib**−**Ie** could be attributed to the effectively reduced conjugation and capability of charge transfer complex formation by aliphatic diacids with the electron-donating diamine moiety in comparison with that of the strongly electron-accepting aromatic diacids. The cutoff wavelengths (λ_0) from UV−vis transmittance spectra were in the range 385−433 nm (Figure S12.)

The electrochemical behavior of compounds **4** and **5** and the polyamide **I** series was investigated by cyclic voltammetry. Compounds were dissolved in dry acetonitrile (10^{-3} M) containing 0.1 M of TBAP as an electrolyte under a nitrogen atmosphere, and the polymers conducted by film cast on an ITO-coated glass substrate as the working electrode in dry acetonitrile containing 0.1 M of TBAP as an electrolyte. The typical cyclic voltammograms for compounds **4** and **5** are shown in Figure 5. Compound **4** showed two reversible oxidation redox couples at $E_{1/2}$ = 0.66, 0.88 V (E_{onset} = 0.58 V) and one irreversible oxidation peak at 1.37 V and exhibited one reversible reduction redox couple at $E_{1/2}$ = −1.14 V. Compound **5** showed five reversible oxidation redox couples at $E_{1/2}$ = 0.30, 0.50, 0.77, 0.97, and 1.41 V (E_{onset} = 0.22). Polymers **Ia**−**Ie** exhibited three reversible oxidation redox couples ($E_{1/2}$) at 0.39−0.47, 0.64−0.72, and 1.02−1.13 V, respectively, versus Ag/AgCl in acetonitrile solution, and **Ie** showed additional fourth reversible oxidation redox couples at 1.07 V (Figure 6). As the substituent varies from electron-withdrawing ($-NO_2$) to electron-donating ($-NH_2$) group, the onset oxidation potential of compound **5** occurred at less positive potential by 0.36 V than compound **4**. It reflects the sensitivity of the reduction/oxidation (redox) reaction to the electronic effect of the substituent. Noticeably, the first, second, and third half-wave oxidation potentials of compound **4** occurred at more positive potentials by 0.36, 0.38, and 0.40 V than compound **5**, respectively. Furthermore, the first, second, and

Table 3. Electrochemical Properties of the Polyamides

polymer code	oxidation (V) E_{onset}	$E_{1/2(ox,1)}$	$E_{1/2(ox,2)}$	$E_{1/2(ox,3)}$	$E_{1/2(ox,4)}$	$E_{1/2(ox,5)}$	reduction (V) E_{onset}	$E_{1/2(red,1)}$	HOMO[b]	LUMO[c]	E_g^{opt} [d]
4	0.58	0.66	0.88	1.37[a]	–[f]	–	−1.05	−1.14	4.94	2.79	2.15 (1.63)[e]
5	0.22	0.30	0.50	0.77	0.97	1.41	–	–	4.58	–	–
Ia	0.26	0.39	0.64	1.05	–	–	–	–	4.62	1.55	3.07
Ib	0.28	0.42	0.68	1.13	–	–	–	–	4.64	1.87	2.77
Ic	0.25	0.39	0.65	1.03	–	–	–	–	4.61	1.61	3.00
Id	0.30	0.47	0.72	1.12	–	–	–	–	4.66	1.74	2.92
Ie	0.27	0.42	0.67	1.02	1.07	–	–	–	4.63	1.79	2.84

[a] Irreversible peak potential. [b] The HOMO energy levels were calculated from cyclic voltammetry and were referenced to ferrocene (4.8 eV). [c] LUMO = HOMO − E_g^{opt}. [d] E_g^{opt} = 1240/λ_{onset}. [e] $E_g^{EC} = E_{onset(ox)} - E_{onset(red)}$. [f] Nondetectable.

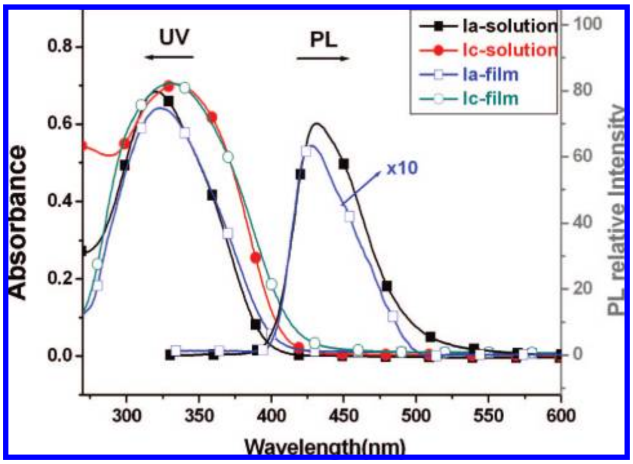

Figure 4. UV−vis absorptions and PL spectra of polyamides **Ia** and **Ic** in NMP (10^{-5} M) and films. Quinine sulfate dissolved in 1 N H_2SO_4(aq) with a concentration of 10^{-5} M as the standard (Φ_F = 0.546).

third half-wave oxidation potentials of polyamide **Ia**−**Ie** occurred between compounds **4** and **5**. Because of the stability of the films and the good adhesion between the polymer and ITO substrate, polyamide **Ic** exhibited excellent reversibility of electrochromic characteristics in 500 continuous cyclic scans between 0.00 and 0.85 V, changing color from colorless to yellow and then blue at applied potentials ranging over 0.55 and 0.80 V. The first electron removal for polyamide **Ic** was assumed to occur at the N atom on one of the 4-amide-4′-methoxydiphenylamino groups, which was more electron richer. The introduction of electron-donating 4-amide-4′-methoxydiphenylamine not only could greatly prevent the coupling reaction but also lower the oxidation potentials. The energy of the highest occupied molecular orbital (HOMO) and lowest unoccupied molecular orbital (LUMO) levels of the investigated polyamides could be determined from the oxidation onset or half-wave potentials and the onset absorption wavelength of polymer films, and the results are listed in Table 4. The oxidation onset potential for **Ic** has been determined as E_{onset} = 0.25 V vs Ag/AgCl. The external ferrocene/ferrocenium (Fc/Fc$^+$) redox standard $E_{1/2}$ is 0.44 V vs Ag/AgCl in CH_3CN. Assuming that the HOMO energy for the Fc/Fc$^+$ standard is 4.80 eV with respect to the zero vacuum level, the HOMO energy for **Ic** was estimated to be 4.61 eV. The film onset absorption value is 414 nm, and estimated optical band gap of the **Ic** is around 3.00 eV.

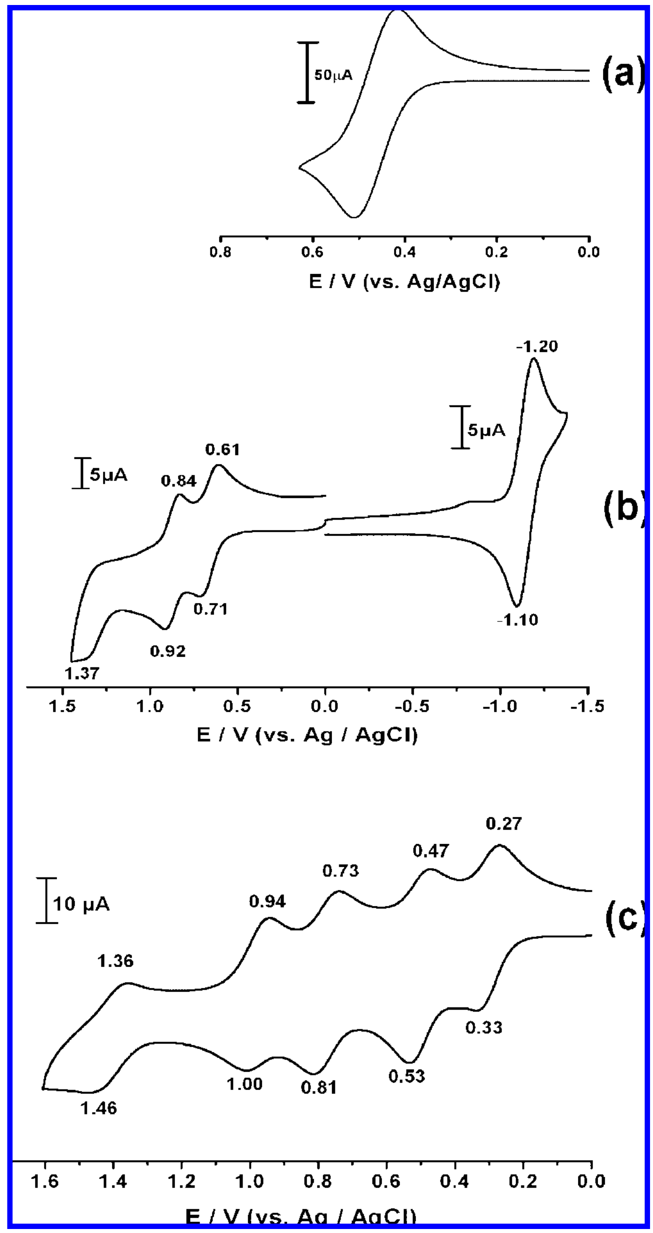

Figure 5. Cyclic voltammograms of 10^{-3} M compounds **4** and **5** in CH_3CN containing 0.1 M TBAP. Scan rate = 0.05 V/s. (a) Ferrocene, (b) compound **4**, and (c) compound **5** oxidation redox.

Electrochromic Characteristics. Electrochromism of compound **4** and the **Ic** thin film was examined by an optically transparent thin-layer electrode (OTTLE) coupled with UV−vis/NIR spectroscopy. The electrode preparations and solution conditions were identical to those used in cyclic voltammetry. Figure 7 shows the spectral changes for compound **4** at various electrode potentials. The absorption peaks at 314 and 418 nm are characteristic for compound **4**. After one-electron oxidation (0.00−0.77 V), the original peaks decreased gradually, and a very broad and intense new band around 1173 nm appeared as shown in Figure 7A. The first oxidation reversibility was 99% based on the absorbance at 314 nm.[21] When the potential was adjusted to more positive values (0.77−0.96 V) corresponding to the second electron oxidation, the spectral change was shown

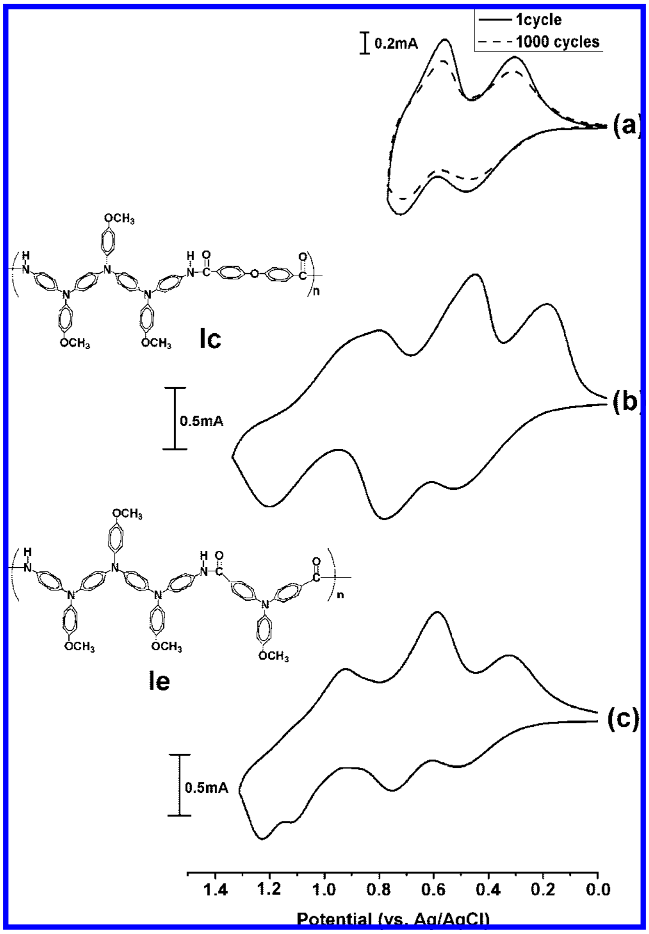

Figure 6. Cyclic voltammograms of (a) polyamide **Ic** film over 1000 cyclic scanning, (b) **Ic**, and (c) **Ie** film onto an indium−tin oxide (ITO)-coated glass substrate in CH_3CN containing 0.1 M TBAP at scan rate = 0.05 V/s.

Table 4. Optical and Electrochemical Data Collected for Coloration Efficiency Measurements of Polyamide Ic

cycles[a]	$\Delta OD\lambda_{443}$[b] (λ_{1080})[c]	ΔT (%) λ_{443} (λ_{1080})	Q (mC/cm^2)[d] first (second)	η (cm^2/C)[e] first (second)	decay (%)[f] first (second)
1	0.394 (0.678)	59.64 (79.02)	1.94 (2.61)	203 (260)	0.00 (0.00)
50	0.394 (0.678)	59.63 (79.02)	1.94 (2.61)	203 (260)	0.00 (0.00)
100	0.394 (0.678)	59.64 (79.02)	1.94 (2.61)	203 (260)	0.00 (0.00)
150	0.394 (0.678)	59.64 (79.02)	1.95 (2.61)	202 (260)	0.49 (0.00)
200	0.394 (0.669)	59.63 (78.57)	1.95 (2.61)	202 (256)	0.49 (1.54)
250	0.394 (0.669)	59.64 (78.57)	1.95 (2.62)	202 (255)	0.49 (1.92)
300	0.394 (0.664)	59.64 (78.32)	1.95 (2.62)	202 (253)	0.49 (2.69)
350	0.390 (0.664)	59.26 (78.32)	1.94 (2.62)	201 (253)	0.99 (2.69)
400	0.386 (0.659)	58.66 (78.01)	1.94 (2.62)	199 (251)	1.94 (3.46)
450	0.382 (0.655)	58.28 (77.87)	1.94 (2.62)	197 (250)	2.96 (3.85)
500	0.377 (0.645)	57.11 (77.36)	1.94 (2.62)	194 (246)	4.44 (5.39)

[a] Times of cyclic scan by applying potential steps: 0.00 ↔ 0.55 (λ_{443}) and 0.00 ↔ 0.80 (λ_{1080}) (V vs Ag/AgCl). [b] Optical density change at 443 nm for **Ic**. [c] Optical density change at 1080 nm for **Ic**. [d] Ejected charge, determined from the in situ experiments. [e] Coloration efficiency is derived from the equation: $\eta = \Delta OD/Q$. [f] Decay of coloration efficiency after cyclic scans.

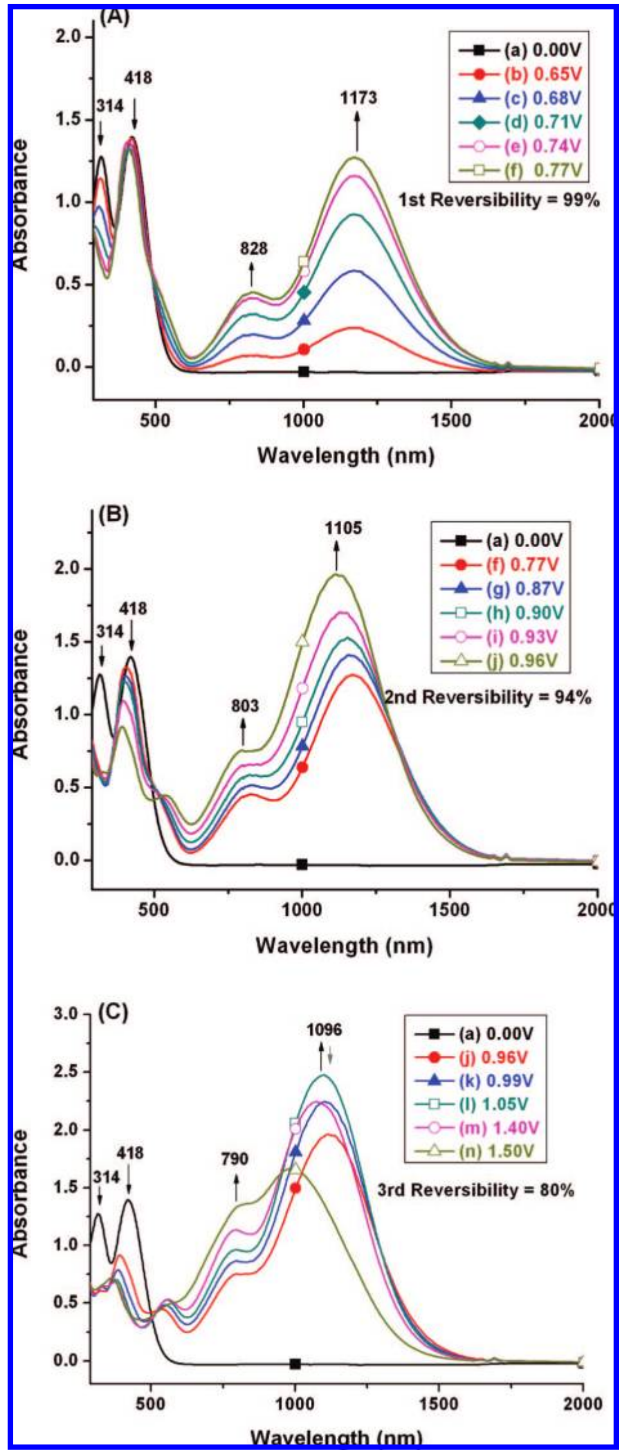

Figure 7. Absorption spectral change of compound **4** (10^{-4} M) in CH_3CN containing 0.1 M TBAP. (A) E_{appl}: (a) 0.00, (b) 0.65, (c) 0.68, (d) 0.71, (e) 0.74, and (f) 0.77 V. (B) E_{appl}: (g) 0.87, (h) 0.90, (i) 0.93, and (j) 0.96 V. (C) E_{appl}: (k) 0.99, (l) 1.05, (m) 1.40, and (n) 1.50 V.

as in Figure 7B. The characteristic new peaks at 803 and 1105 nm appeared and the second oxidation reversibility was 94%. It shows that the first and second oxidations are reversible with high stability. When the applied potential was adding to 1.50 V, the characteristic peaks' new bands at 790 and 1096 nm appeared (Figure 7C), but only 80% absorbance remained, implying that the oxidation product (trication) was not stable. The same experiment for polyamide **Ic** film exhibited the first, second, and third oxidation reversibility up to 100%, 99%, and 75%, respectively, as shown in Figure 8.

All these polyamides exhibited similar electrochromic properties, and the typical electrochromic transmittance spectra of polyamide **Ic** are shown in Figure 9. When the applied potentials increased positively from 0.00 to 0.55 V, the characteristic peak of transmittance at 326 nm for polyamide **Ic** neutral form decreased gradually, while two new bands grew up at 443 and 1080 nm due to the first stage oxidation. When the potential was adjusted to a more positive value of 0.80 V, corresponding to the second step oxidation, the peak of characteristic absorbance (326, 443 nm) decreased gradually while two new band

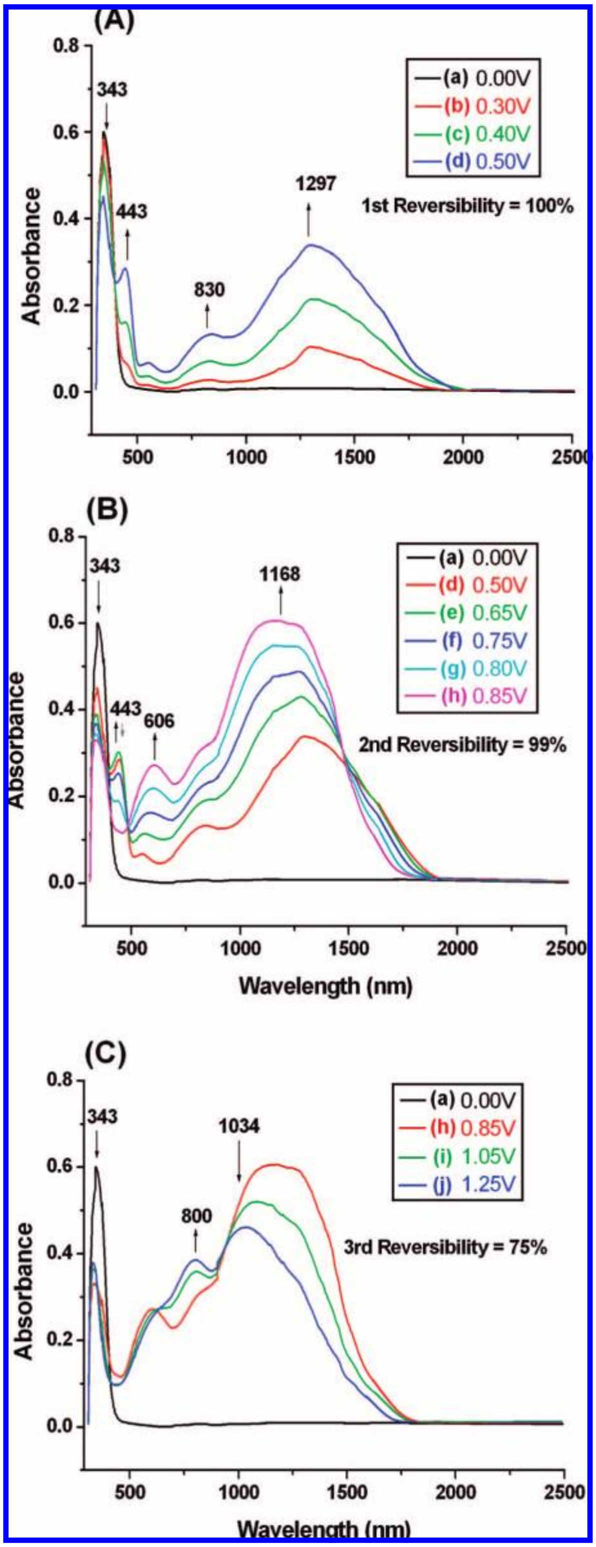

Figure 8. Absorption spectral change of polyamide **Ic** thin film (in CH_3CN with 0.1 M TBAP as the supporting electrolyte) (A) E_{appl}: (a) 0.00, (b) 0.30, (c) 0.40, and (d) 0.50 V. (B) E_{appl}: (e) 0.65, (f) 0.75, (g) 0.80, and (h) 0.85 V. (C) E_{appl}: (i) 1.05 and (j) 1.25 V.

grew up at 590 and 1080 nm. By applying positive potential value up to 1.25 V, corresponding to the third step oxidation, the peak of characteristic absorbance (1080 nm) decreased gradually while one new band grew up at 831 nm. Meanwhile, the film of polymer **Ic** changed from original colorless to yellow and then to a blue oxidized form and also exhibited highly contrast of optical transmittance change (ΔT %) up to 59% at 443 nm for yellow (first oxidation), 79% at 1080 nm for blue

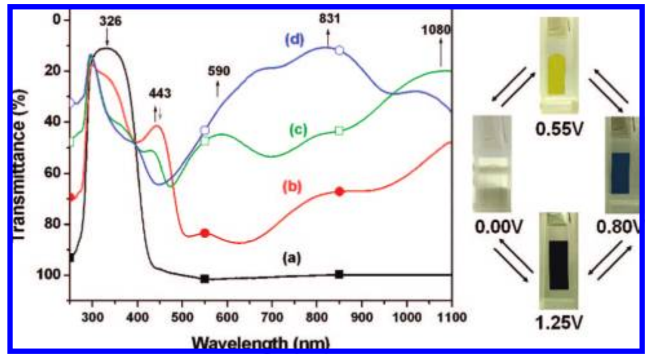

Figure 9. Electorchromic behavior of polyamide **Ic** thin film (in CH_3CN with 0.1 M TBAP As the supporting electrolyte) at (a) 0.00, (b) 0.55, (c) 0.80 and (d) 1.25 (V vs Ag/AgCl).

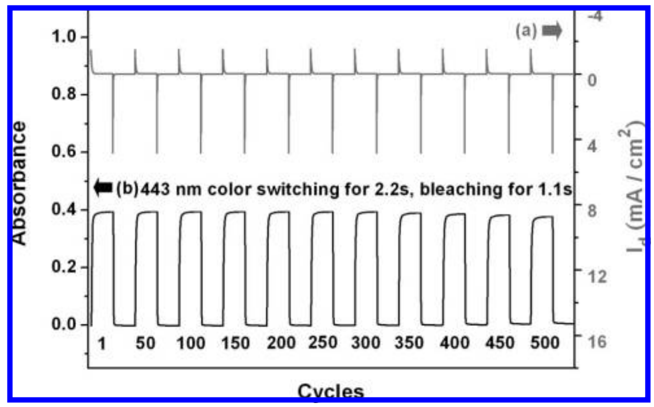

Figure 10. (a) Current consumption and (b) potential step absorptometry of polyamide **Ic** (in CH_3CN with 0.1 M TBAP as the supporting electrolyte) by applying a potential step (0.00 V $\leftrightarrows$ 0.55 V), (coated area: 1 cm^2) and cycle time 120 s for coloration efficiency from 203 cm^2/C (1st cycle) to 194 cm^2/C (500th cycle).

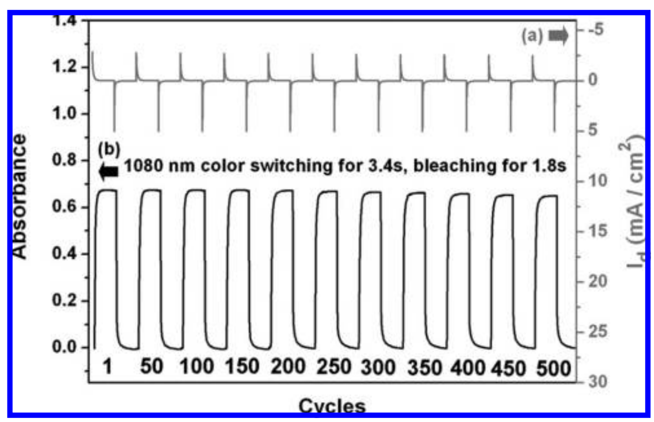

Figure 11. (a) Current consumption and (b) potential step absorptometry of polyamide **Ic** (in CH_3CN with 0.1 M TBAP as the supporting electrolyte) by applying a potential step (0.00 V $\leftrightarrows$ 0.80 V), (coated area: 1 cm^2) and cycle time 120 s for coloration efficiency from 260 cm^2/C (1st cycle) to 246 cm^2/C (500th cycle).

(second oxidation), and 88% at 831 nm for deep blue (third oxidation).

The color switching times were estimated by applying a potential step, and the absorbance profiles are shown in Figures 10 and 11. The switching time was defined as the time required for reach 90% of the full change in absorbance after the switching of the potential. Polyamide **Ic** thin film required 2.2 s at 0.55 V for color switching and only 1.0 s for bleaching (Figure 10). When the potential was set at 0.80 V, the thin film required 3.4 s for coloration and 1.8 s for bleaching (Figure

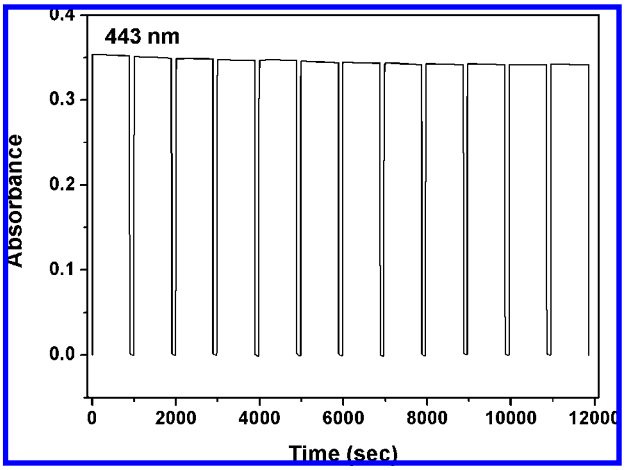

Figure 12. Potential step absorptometry of polyamide **Ic** (in CH_3CN with 0.1 M TBAP as the supporting electrolyte) by applying a potential step (0.00 V ⇆ 0.55 V) under a cycle time of on and off for 900 and 100 s, respectively.

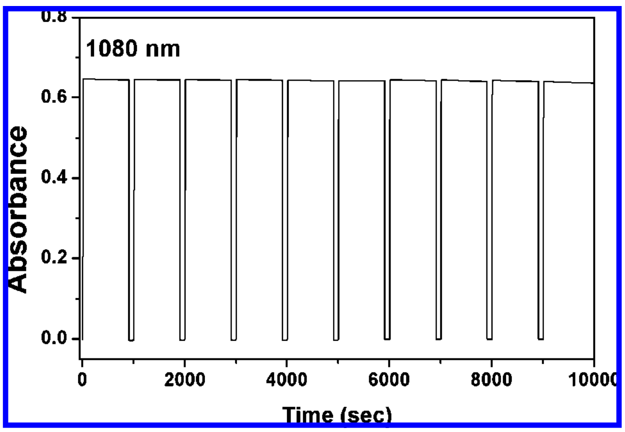

Figure 13. Potential step absorptometry of polyamide **Ic** (in CH_3CN with 0.1 M TBAP as the supporting electrolyte) by applying a potential step (0.00 V ⇆ 0.80 V) under a cycle time of on and off for 900 and 100 s, respectively.

11). The high electrochromic coloration efficiency and low decay of the polyamide **Ic** for yellow ($\eta = \Delta OD_{443}/Q$) (203 cm^2/C for 1 cycle to 194 cm^2/C for 500 cycles), blue ($\eta = \Delta OD_{1080}/Q$) (260 cm^2/C for 1 cycle to 246 cm^2/C for 500 cycles), and deep blue ($\eta = \Delta OD_{831}/Q$) (297 cm^2/C for 1 cycle to 255 cm^2/C for 100 cycles) could be obtained and calculated,[22] and the results are summarized in Tables 4 and S2. Figures 12 and 13 show the long-term stability test by keeping 15 min for each switching on at potential 0.55 and 0.80 V, respectively, and also exhibited highly stable electrochromic behaviors.

Conclusions

A series of highly stable anodic electrochromic polyamides with high contrast of optical transmittance change have been readily prepared from the new diamine 4,4′-bis[4-aminophenyl(4-methoxyphenyl)amino]-4′′-methoxytriphenylamine and various dicarboxylic acids via the direct polycondensation. By incorporation of electron-donating methoxy substituents at the *para* position of TPA moieties, oxidative coupling reaction could not only be greatly prevented by affording stable cationic radicals but also effectively lower the oxidation potentials of the electroactive polyamides. These anodically polymeric electrochromic materials also showed excellent continuous cyclic stability of electrochromic characteristic with good coloration efficiency of yellow (203 cm^2/C for 1 cycle to 194 cm^2/C for 500 cycles) and blue (260 cm^2/C for 1 cycle to 246 cm^2/C for 500 cycles), changing color from the colorless or pale yellowish neutral form to the yellow and blue oxidized forms when scanning potentials positively from 0.00 to 0.80 V. After over 500 cyclic switches, the polymer films still exhibited excellent reversibility of electrochromic characteristics. Thus, these novel TPA-containing polyamides have a great potential as a new type of hole-transporting and electrochromic materials due to their proper HOMO values as well as excellent electrochemical and thermal stability.

Acknowledgment. The authors are grateful to the National Science Council of the Republic of China for financial support of this work.

Supporting Information Available: Text giving experimental data, including synthesis of the monomers and diagrams showing their structures, figures showing ^{1}H and ^{13}C NMR spectra, COSY spectra, HMQC spectra, IR spectra, UV−vis absorption spectra, PL spectra, WAXD patterns, transmission UV−vis absorption spectra, and a table giving optical properties data. This material is available free of charge via the Internet at http://pubs.acs.org.

References and Notes

(1) (a) Monk, P. M. S.; Mortimer, R. J.; Rosseinsky, D. R. *Electrochromism: Fundamentals and Applications*; VCH: Weinheim, Germany, 1995. (b) Monk, P. M. S.; Mortimer, R. J.; Rosseinsky, D. R. *Electrochromism and Electrochromic Devices*; Cambridge University Press: Cambridge, UK, 2007. (c) Rosseinsky, D. R.; Mortimer, R. J. *Adv. Mater.* **2001**, *13*, 783.
(2) (a) Granqvist, C. G.; Azens, A.; Isidorsson, J.; Kharrazi, M.; Cullman, L.; Lindstroem, T.; Niklasson, G. A.; Ribbing, C. G.; Roennow, D.; Stromme Mattsson, M.; Veszelei, M. *J. Non-Cryst. Solids* **1997**, *218*, 273. (b) Byker, H. J. Gentex Corporation, U.S. Patent No. 4902108. (c) Mortimer, R. G. *Chem. Soc. Rev.* **1997**, *26*, 147.
(3) (a) Monk, P. M. S. *J. Electroanal. Chem.* **1997**, *432*, 175. (b) Bange, K. *Sol. Energy Mater. Sol. Cells* **1999**, *58*, 1.
(4) (a) Granqvist, C. G.; Azens, A.; Hjelm, A.; Kullman, L.; Niklasson, G. A.; Ribbing, C. G.; Roennow, D.; Stromme Mattsson, M.; Veszelei, M.; Vaivars, G. *Sol. Energy* **1998**, *63*, 199. (b) Rauh, R. D. *Electrochim. Acta* **1999**, *44*, 3165. (c) Tracy, C. E.; Zhang, J. G.; Benson, D. K.; Czanderna, A. W.; Deb, S. K. *Electrochim. Acta* **1999**, *44*, 3195. (d) Pennisi, A.; Simone, F.; Barletta, G.; Di Marco, G.; Lanza, M. *Electrochim. Acta* **1999**, *44*, 3237.
(5) (a) Meeker, D. L.; Mudigonda, D. S. K.; Osborn, J. M.; Loveday, D. C.; Ferraris, J. P. *Macromolecules* **1998**, *31*, 2943. (b) Mudigonda, D. S. K.; Meeker, D. L.; Loveday, D. C.; Osborn, J. M.; Ferraris, J. P. *Polymer* **1999**, *40*, 3407. (c) Brotherston, I. D.; Mudigonda, D. S. K.; Osborn, J. M.; Belk, J.; Chen, J.; Loveday, D. C.; Boehme, J. L.; Ferraris, J. P.; Meeker, D. L. *Electrochim. Acta* **1999**, *44*, 2993.
(6) Dautremont-Smith, W. C. *Displays I* **1982**, 3.
(7) Mortimer, R. J. *Electrochim. Acta* **1999**, *44*, 2971.
(8) Bange, K.; Bambke, T. *Adv. Mater.* **1990**, *2*, 10.
(9) (a) Sapp, S. A.; Sotzing, G. A.; Reynolds, J. R. *Chem. Mater.* **1998**, *10*, 2101. (b) Kumar, A.; Welsh, D. M.; Morvant, M. C.; Piroux, F.; Abboud, K. A.; Reynolds, J. R. *Chem. Mater.* **1998**, *10*, 896.
(10) (a) Thompson, B. C.; Schottland, P.; Zong, K.; Reynolds, J. R. *Chem. Mater.* **2000**, *12*, 1563. (b) Thompson, B. C.; Schottland, P.; Sonmez, G.; Reynolds, J. R. *Synth. Met.* **2001**, *119*, 333.
(11) (a) Skotheim, T. A.; Elsenbaumer, R. L.; Reynolds, J. R. *Handbook of Conducting Polymers*, 2nd ed.; Marcel Dekker: New York, 1998. (b) NalwaH. S. *Handbook of Organic Conductive Molecules and Polymers*; John Wiley and Sons: New York, 1997. (c) Sonmez, G.; Schwendeman, I.; Schottland, P.; Zong, K.; Reynolds, J. R. *Macromolecules* **2003**, *36*, 639. (d) Schwendeman, I.; Hickman, R.; Sonmez, G.; Schottland, P.; Zong, K.; Welsh, D.; Reynolds, J. R. *Chem. Mater.* **2002**, *14*, 3118.
(12) Seo, E. T.; Nelson, R. F.; Fritsch, J. M.; Marcoux, L. S.; Leedy, D. W.; Adams, R. N. *J. Am. Chem. Soc.* **1966**, *88*, 3498.
(13) (a) Ito, A.; Ino, H.; Tanaka, K.; Kanemoto, K.; Kato, T. *J. Org. Chem.* **2002**, *67*, 491. (b) Chiu, K. Y.; Su, T. H.; Li, J. H.; Lin, T. H.; Liou, G. S.; Cheng, S. H. *J. Electroanal. Chem.* **2005**, *575*, 95.
(14) (a) Cassidy, P. E. *Thermally Stable Polymers*; Marcel Dekker: New York, 1980. (b) Yang, H. H. *Aromatic High-Strength Fibers*; Wiley: New York, 1989.
(15) (a) Hsiao, S. H.; Li, C. T. *Macromolecules* **1998**, *31*, 721. (b) Liou, G. S. *J. Polym. Sci., Part A: Polym. Chem.* **1998**, *36*, 1937. (c)

Eastmond, G. C.; Gibas, M.; Paprotny, J. *Eur. Polym. J.* **1999**, *35*, 2097. (d) Myung, B. Y.; Ahn, C. J.; Yoon, T. H. *Polymer* **2004**, *45*, 3185.
(16) (a) Liou, G. S.; Hsiao, S. H.; Ishida, M.; Kakimoto, M.; Imai, Y. *J. Polym. Sci., Part A: Polym. Chem.* **2002**, *40*, 2810. (b) Liou, G. S.; Hsiao, S. H.; Ishida, M.; Kakimoto, M.; Imai, Y. *J. Polym. Sci., Part A: Polym. Chem.* **2002**, *40*, 3815. (c) Liou, G. S.; Hsiao, S. H. *J. Polym. Sci., Part A: Polym. Chem.* **2003**, *41*, 94. (d) Hsiao, S. H.; Chen, C. W.; Liou, G. S. *J. Polym. Sci., Part A: Polym. Chem.* **2004**, *42*, 3302.
(17) (a) Cheng, S. H.; Hsiao, S. H.; Su, T. H.; Liou, G. S. *Macromolecules* **2005**, *38*, 307. (b) Su, T. H.; Hsiao, S. H.; Liou, G. S. *J. Polym. Sci., Part A: Polym. Chem.* **2005**, *43*, 2085. (c) Liou, G. S.; Hsiao, S. H.; Su, T. H. *J. Mater. Chem.* **2005**, *15*, 1812. (d) Chang, C. W.; Liou, G. S.; Hsiao, S. H. *J. Mater. Chem.* **2007**, *17*, 1007.
(18) Liou, G. S.; Chang, C. W. *Macromolecules* **2008**, *41*, 1667.
(19) Demas, J. N.; Crosby, G. A. *J. Phys. Chem.* **1971**, *75*, 991.
(20) (a) Yamazaki, N.; Higashi, F.; Kawabata, J. *J. Polym. Sci., Polym. Chem. Ed.* **1974**, *12*, 2149. (b) Yamazaki, N.; Matsumoto, M.; Higashi, F. *J. Polym. Sci., Polym. Chem. Ed.* **1975**, *13*, 1373.
(21) Chiu, K. Y.; Su, T. H.; Huang, C. W.; Liou, G. S.; Cheng, S. H. *J. Electroanal. Chem.* **2005**, *578*, 283.
(22) Mortimer, R. J.; Reynolds, J. R. *J. Mater. Chem.* **2005**, *15*, 2226.

MA8021019